ACS OMEGA

http://pubs.acs.org/journal/acsodf

Article

Novel Analogues of the Chikungunya Virus Protease Inhibitor: Molecular Design, Synthesis, and Biological Evaluation

Larisa Ivanova, Kai Rausalu, Maksim Ošeka, Dzmitry G. Kananovich, Eva Žusinaite, Jaana Tammiku-Taul, Margus Lopp, Andres Merits,* and Mati Karelson*

Cite This: *ACS Omega* 2021, 6, 10884−10896

Read Online

ACCESS | Metrics & More | Article Recommendations | Supporting Information

ABSTRACT: The Chikungunya virus (CHIKV) is an arbovirus belonging to the genus *Alphavirus* of the *Togaviridae* family. CHIKV is transmitted by the mosquitoes and causes Chikungunya fever. CHIKV outbreaks have occurred in Africa, Asia, Europe, and the countries of Indian and Pacific Oceans. In 2013, CHIKV cases were registered for the first time in the Americas on the Caribbean islands. There is currently no vaccine to prevent or medicines to treat CHIKV infection. The CHIKV nonstructural protease (nsP2) is a promising potential target for the development of drugs against CHIKV infection because this protein is one of the key components of the viral replication complex and is involved in multiple steps of virus infection. In this work, novel analogues of the potential CHIKV nsP2 protease inhibitor, first reported by Das et al. in 2016, were identified using molecular modeling methods, synthesized, and evaluated *in vitro*. The optimization of the structure of the inhibitor allowed to increase the antiviral activity of the compound 2−10 times. The possible mechanism of action of the identified potential inhibitors of the CHIKV nsP2 protease was studied in detail using molecular dynamics (MD) simulations. According to the MD results, the most probable mechanism of action is the blocking of conformational changes in the nsP2 protease required for substrate recognition and binding.

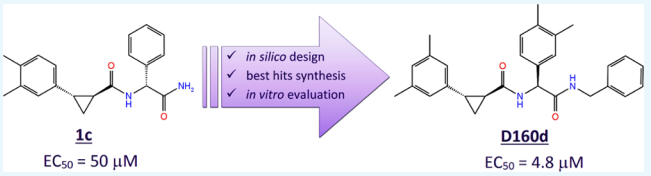

INTRODUCTION

The Chikungunya virus (CHIKV) is an arbovirus of the genus *Alphavirus* of the *Togaviridae* family. CHIKV is spread by two mosquito species: *Aedes aegypti* and *Aedes albopictus*. Chikungunya fever, a disease caused by CHIKV infection in humans, usually lasts 5 to 7 days and is rarely life-threatening (the risk of death is around 1 case per 1000).[1] However, it often results in severe long-lasting (months to years) joints' dysfunction.[2] There is no specific treatment for this disease, but nonsteroid anti-inflammatory drugs may be used to relieve pain and joint swelling. There is also no vaccine against CHIKV; therefore, the protective measures include the prevention of mosquito bites and destroying mosquito breeding sites. Global rates of CHIKV infection vary by the outbreak. When the virus was first discovered in West Africa in 1952,[3] the spread of the virus was low. Since the 1960s, periodic outbreaks have been reported in Asia and Africa.[4] However, since 2005, CHIKV has repeatedly re-emerged and caused major outbreaks in Africa, Asia, and America. In India, the virus reappeared after 32 years.[5] Outbreaks have also been reported in previously unreported areas of CHIKV: Europe, the Caribbean, and South America. Local distribution has also been recorded in the United States and Australia.[6] In 2005, the outbreak on the la Réunion island was the largest at that time: an estimated 266,000 cases were recorded on the island with a population of about 770,000.[7] In 2006, 1.25 million cases were reported during the Indian outbreak.[8] The sharp increase and expansion of the CHIKV incidence in recent years testify to our vulnerability to emerging infectious diseases transmitted by insects and emphasize the importance of finding effective drugs to treat such diseases.

CHIKV has small (∼70 nm in diameter) virions and a positive-sense RNA genome of approximately 11.6 kb. The genome contains two open reading frames encoding for nonstructural proteins (nsP1−nsP4) and structural proteins (C, E3, E2, E1, and 6K).[9,10] Among CHIKV nonstructural proteins, which represent subunits of virus-encoded RNA replicase, nsP2 is the most attractive target for the development of new antiviral drugs. Aside its functions in virus RNA replication, it is also important for shutdown of the host cell transcription, inhibition of antiviral responses, and virion formation; most of these functions are associated with the C-terminal protease part of nsP2.[11]

In recent years, many research groups have focused on identifying new inhibitors of CHIKV replication in order to develop a candidate drug for the treatment of CHIKV infection, as described in review articles by Subudhi et al.[4]

Received: February 3, 2021
Accepted: April 2, 2021
Published: April 14, 2021

Scheme 1. Most Active CHIKV Protease Inhibitor 1c from the Previous Study (Das et al. 2016), Its *In Silico* Modeled Analogues Designed for This Work and Chemical Synthesis of the Best Hits for Evaluation of Bioactivity

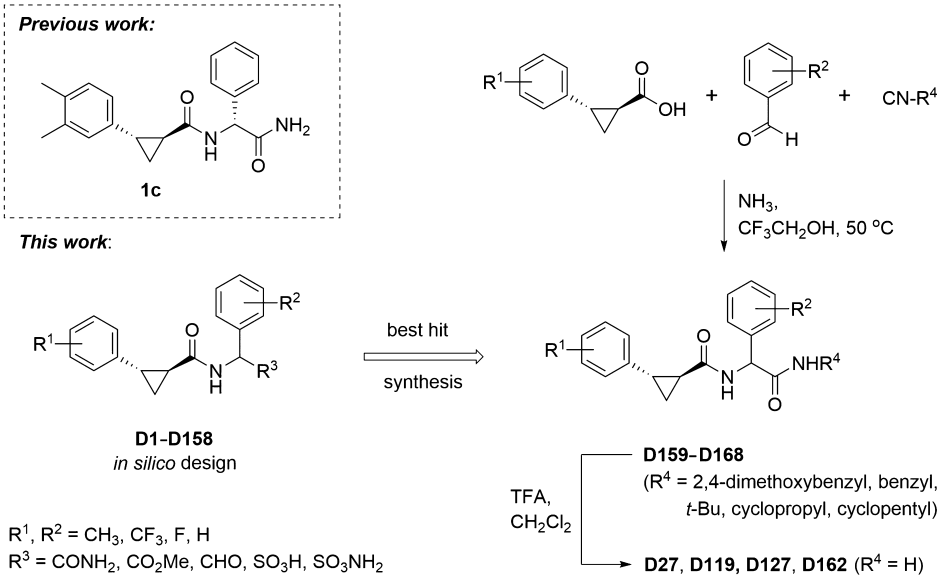

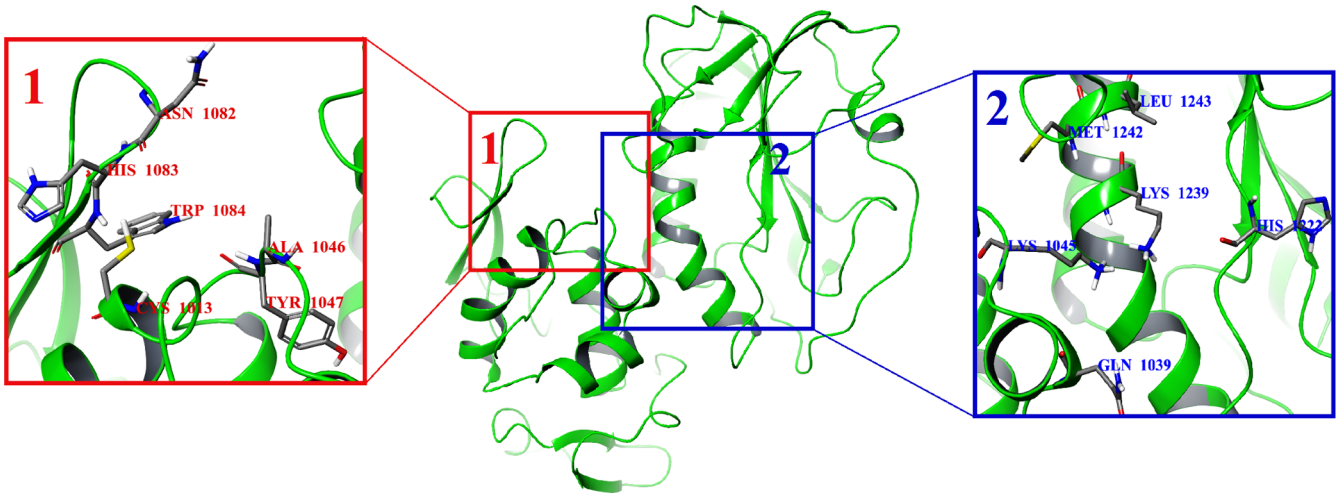

Figure 1. Potential binding sites **1** and **2** in the CHIKV nsP2 protease (PDB ID: 3TRK).

and Jadav et al.[12] The use of computer-aided drug design (CADD) methods helps to accelerate the long process of developing new drug candidates and reduce their cost. In our previous work,[13] a compound originating from the study by Bassetto et al.[14] was selected as the lead structure for hit generation to identify novel inhibitors against the CHIKV nsP2 protease, combining CADD based on molecular docking, molecular dynamics (MD) simulations, and the pharmacophore approach with the use of cell-free and cell-culture experiments. The aim of our current study was to optimize the structure and increase the antiviral properties of the previously reported CHIKV nsP2 inhibitor[13] (Scheme 1) using the structure–activity relationship for the newly designed and synthesized compounds.

RESULTS AND DISCUSSION

Molecular Design and Molecular Docking. In this work, the CHIKV nonstructural protease nsP2 (PDB ID: 3TRK;[15] see the Materials and Methods section) was used as a target for molecular design. Two potential binding sites of the CHIKV nsP2 protease were used for molecular docking (Figure 1). To search for more active analogues of the previously described inhibitor,[13] 158 compounds were designed modifying substituents and their positions in the phenyl rings (Scheme 1). It was shown in the previous work[13] that only the relative configuration of cyclopropane substituents (*trans*-configuration) has an important role in the antiviral activity of *trans*-2-{[2-(3,4-dimethylphenyl)-cyclopropyl]formamido}-2-phenylacetamide (**1c**), while the absolute configuration of the cyclopropane motif and the stereocenter of arylglycine do not impose any significant effect on the activity. According to these results, the *S*,*S*,*S*-stereoisomers of designed compounds were used for the molecular docking study, and during this procedure, only the cyclopropane substituents were fixed in the *trans*-configuration for all compounds, while the other bonds in the molecules were marked as flexible. The active site (hereinafter referred to as potential binding site **1**; Figure 1) from the previous work,[13] including the amino acid residues Cys1013 and His1083 (hereinafter, the numbers of amino acid residues correspond to

https://doi.org/10.1021/acsomega.1c00625
ACS Omega 2021, 6, 10884–10896

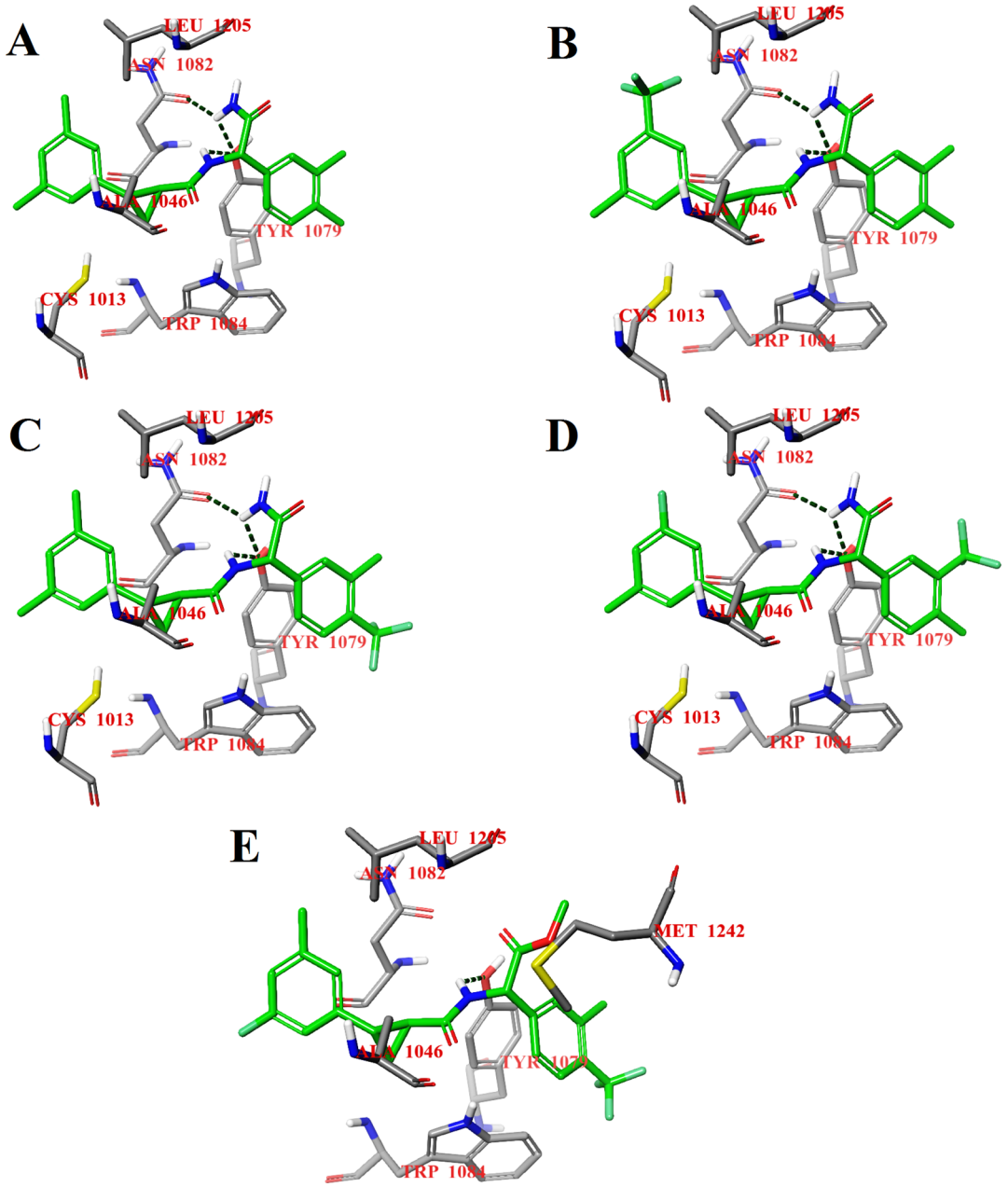

Figure 2. Calculated binding modes of the *S*,*S*,*S*-stereoisomers of compounds **D27** (A), **D117** (B), **D120** (C), **D127** (D), and **D157** (E) at potential binding site **1** of CHIKV nsP2 (PDB ID: 3TRK). Intermolecular hydrogen bonds are shown by dark-green dashed lines.

their numbers in the nonstructural polyprotein of CHIKV) from the catalytic dyad and the conserved amino acid residue Trp1084, was chosen for the docking calculations. However, the number of selected compounds based on the calculated binding energy hits for the *S*,*S*,*S*-stereoisomers of designed compounds turned out to be too large (121 hits from 158 compounds; Table S1). An *S*,*S*,*S*-stereoisomer of the designed compound with a binding energy lower than or equal to −8.0 kcal/mol[16] was considered as a binding energy hit. Thus, the binding energies of the selected hits for this active site were in the range of −9.4 to −8.0 kcal/mol. Therefore, another potential active site of CHIKV nsP2 at the C-terminal (hereinafter referred to as potential binding site **2**; Figure 1) was used for further molecular docking, containing the following amino acids: Gln1039, Lys1045, Glu1157, Gly1176, His1222, Lys1239, Ser1293, Glu1296, and Met1297.[17] The difference in the binding energy of small-molecule ligands with CHIKV nsP2 was not as large as that in the case of potential binding site **1**. Thus, 28 hits from 158 compounds with the binding energies ranging from −8.7 to −8.0 kcal/mol were identified (Table S1). Analysis of the docking results at potential binding site **2** showed that the binding energy of the *S*,*S*,*S*-stereoisomers of designed compounds to the receptor is improved if the substituents R^1 are located at the meta positions of the phenyl ring and R^2 at the meta and para positions of the phenyl ring (see Scheme 1, Table S1).

Compounds **D27**, **D117**, **D120**, **D127**, and **D157** were selected for further study because of the best binding energies of their *S*,*S*,*S*-stereoisomers for both binding sites (Table S1), and compounds **D27** and **D127** were initially selected for synthesis. The calculated binding energies of the *S*,*S*,*S*-

https://doi.org/10.1021/acsomega.1c00625
ACS Omega 2021, 6, 10884−10896

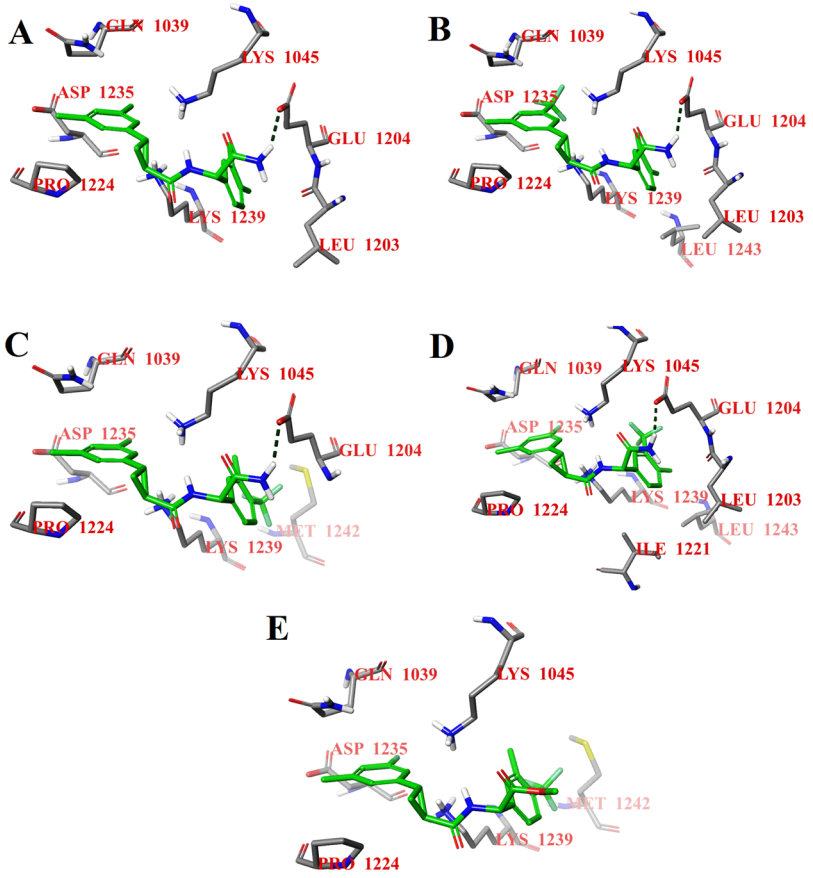

Figure 3. Calculated binding modes of the *S*,*S*,*S*-stereoisomers of compounds **D27** (A), **D117** (B), **D120** (C), **D127** (D), and **D157** (E) at potential binding site **2** of CHIKV nsP2 (PDB ID: 3TRK). Intermolecular hydrogen bonds are shown by dark-green dashed lines.

stereoisomers of selected compounds were in the range of −9.2 to −8.8 kcal/mol for potential binding site **1** and in the range of −8.7 to −8.0 kcal/mol for potential binding site **2**. The choice of the compounds for further study and synthesis also depended on the type and positions of the substituents in the phenyl rings. The binding modes of all *S*,*S*,*S*-stereoisomers of selected compounds at potential binding site **1** of CHIKV nsP2 are the same (Figure 2). The *S*,*S*,*S*-stereoisomers of compounds **D27**, **D117**, **D120**, and **D127** form three hydrogen bonds: one hydrogen bond by the NH_2 group with the OH group of Tyr1079 and another hydrogen bond with the carbonyl oxygen of the side chain of Asn1082; the third hydrogen bond occurs between the NH group of the ligand and the OH group of Tyr1079 (Figure 2A−D). The substitution of the NH_2 group with an OCH_3 group in the *S*,*S*,*S*-stereoisomer of compound **D157** results in the loss of hydrogen bonds with Tyr1079 and Asn1082, but the bond between the NH group of the ligand and the OH group of Tyr1079 is retained (Figure 2E). The loss of two hydrogen bonds causes a small displacement of the ligand at potential binding site **1**, which in turn leads to the loss of a hydrophobic contact with the amino acid residue Cys1013 from the catalytic dyad, but at the same time, it promotes the binding of the ligand closer to the amino acid residue Trp1084, which is important for the CHIKV nsP2 activity.[18]

The binding modes of the *S*,*S*,*S*-stereoisomers of selected compounds also show the same tendency at potential binding site **2** (Figure 3). The *S*,*S*,*S*-stereoisomers of compounds **D27**, **D117**, **D120**, and **D127** are hydrogen-bonded by the terminal NH_2 group to the carboxyl group of Glu1204 (Figure 3A−D). As in the case of potential binding site **1**, the substitution of the terminal NH_2 group by the OCH_3 group also leads to the loss of the hydrogen bond and to a small displacement of the *S*,*S*,*S*-stereoisomer of compound **D157** at potential binding site **2** (Figure 3E) relative to the other selected compounds. As can be seen from the docking results for both potential binding sites of the CHIKV nsP2 protease (Figures 2 and 3), the NH_2 group of the ligand can be the key to the antiviral activity of these compounds. Therefore, it was decided to study the biological activity of intermediates with the substituted terminal NH_2 group (compounds **D159**−**D161**; Scheme 1).

Cytotoxicity of Compounds. First, all synthesized compounds, including intermediates with the substituted terminal NH_2 group, were tested for their cytotoxicity effect in BHK-21 cells; concentrations ranging from 1 to 100 μM were used. To facilitate chemical synthesis and screening for a large array of potential inhibitors, all synthesized compounds were initially tested as equimolecular mixtures of four possible stereoisomers (*R*,*R*,*R*-, *R*,*R*,*S*-, *S*,*S*,*R*-, and *S*,*S*,*S*-stereoisomers). Based on the results of the previous work,[13] we surmised that individual stereoisomers do not interfere with biological activities of each other. Among the intermediates with the substituted terminal NH_2 group, **D161** demonstrated a moderate cytotoxicity effect at a 100 μM concentration, and compounds **D159** and **D160** had no cytotoxic effect at concentrations of 1 up to 100 μM. Among the analogues of compound **D160**, compound **D27** was toxic at all concentrations, compound **D127** showed cytotoxicity at concentrations of more than 100 μM, and compound **D163** showed

https://doi.org/10.1021/acsomega.1c00625
ACS Omega 2021, 6, 10884−10896

cytotoxicity at concentrations of more than 10 μM; the other analogues were nontoxic (Table 1).

Table 1. Antiviral Activity and Cytotoxicity of Synthesized Compounds against CHIKV-NanoLuc in BHK-21 Cells

code	EC_{50} (μM)	CC_{50} (μM)
D27[a]	NA[b]	<0.1
D119[a]	32.0	>100
D127[a]	29.6	>100
D159[a]	>100	>100
D160[a]	10.5	>100
D160a	26.8	>100
D160b	70.7	>100
D160c	8.7	>100
D160d	4.8	>100
D161[a]	13.9	>100
D162[a]	95.9	>100
D163[a]	NA[b]	10
D164[a]	50.5	>100
D165[a]	>100	>100
D166[a]	NA[b]	>100

[a]Compounds were tested as equimolecular mixtures of four possible stereoisomers. [b]NA: inactive, that is, no activity at the maximum nontoxic concentration.

Synthesis of Compounds and Evaluation of Anti-CHIKV Activity. Compounds **D27**, **D119**, **D127**, and **D159**–**D168** were synthesized, as described in the Supporting Information, by using Ugi multi-component reaction as the key step (Scheme 1).[19,20] Since the Ugi reaction was not diastereoselective and racemic 2-arylcyclopropane-1-carboxylic acids were used as starting materials, equimolecular mixtures of four possible stereoisomers (two pairs of enantiomers) were obtained in these cases. Individual stereoisomers were isolated only for compound **D160** with the highest antiviral activity and synthesized from (*R*,*R*)- and (*S*,*S*)-enantiomers (>94% *ee*) of *trans*-2-(3,5-dimethylphenyl)cyclopropane-1-carboxylic acid (see the Supporting Information). Compounds **D159**, **D160**, and **D161** were tested as equimolecular mixtures of four possible stereoisomers (*R*,*R*,*R*-, *R*,*R*,*S*-, *S*,*S*,*R*-, and *S*,*S*,*S*-stereoisomers) for their ability to inhibit CHIKV infection *in vitro* at concentrations of 1 up to 100 μM in BHK-21 cells (Table 1). These compounds behaved differently against CHIKV infection. Compound **D159** was inactive, the inhibitory effect of compounds **D160** and **D161** appeared at a 10 μM concentration, and the viral infection was almost completely inhibited at a 100 μM concentration. However, the inhibitory effect of compound **D161** may be due to its moderate cytotoxic effect at a concentration of 100 μM.

For compounds **D160** and **D161**, 50% effective concentration (EC_{50}) was determined using concentrations from 0.1 up to 200 μM and cells infected at a multiplicity of infection (MOI) of 0.001 using CHIKV-NanoLuc, a marker-protein expressing variant of CHIKV from la Réunion island outbreak. At this low MOI, both compounds showed EC_{50} in the low-micromole range (10.5 and 13.9 μM, respectively). Among the potential inhibitors **D159**, **D160**, and **D161**, the antiviral activity of these compounds was found to depend on their substituents in the terminal NH_2 group. For further biological evaluation of the detected dependence, three analogues of **D160** were synthesized—compounds **D27**, **D163**, and **D164**, which have a different substituent in the terminal NH_2 group. Based on the results of molecular design, compounds **D119**, **D127**, and **D162** with different positions of the methyl and trifluoromethyl groups in the phenyl rings were selected for synthesis. To determine the dependence of the antiviral activity on the position of the methyl substituents R^2 in the corresponding phenyl ring, an analogue of **D159** having the methyl substituents at the meta and para positions (compound **D165**) was first synthesized, followed by its fluoro-substituted derivative **D166**. Among these, compounds **D119**, **D127**, and **D164** were the most active—their EC_{50} were 32.0, 29.6, and 50.5 μM, respectively. Two compounds, **D159** and **D165**, had EC_{50} greater than 100 μM. Other compounds showed no antiviral activity at their maximum nontoxic concentrations (Table 1).

The results of the measurement of the antiviral activity of these compounds confirmed that not only the substituent in the terminal NH_2 group but also the positions of the substituents R^2 in the phenyl ring of arylglycine significantly affect the anti-CHIKV activity. Attachment of a cyclopropyl substituent to the terminal NH_2 group increased cytotoxicity;

Scheme 2. Individual Stereoisomers for Compound D160 with the Denoted Configurations of the Stereocenters[a]

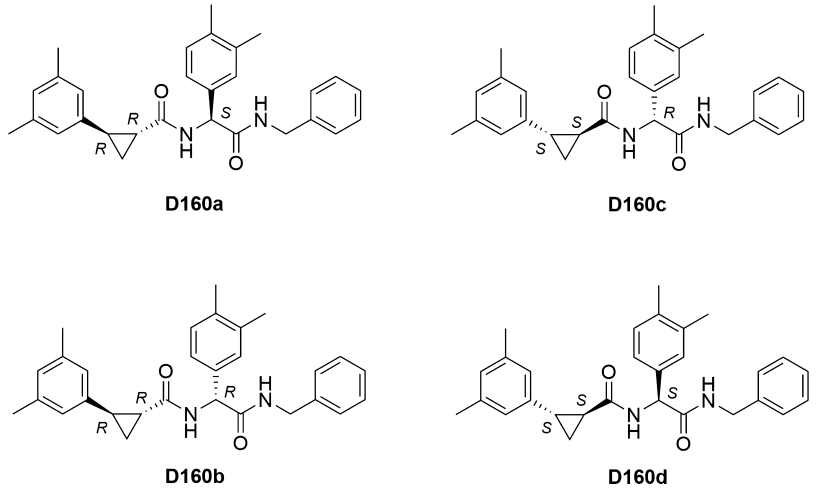

[a]Letters *R* and *S* denote the absolute configurations of the stereocenters.

https://doi.org/10.1021/acsomega.1c00625
ACS Omega 2021, 6, 10884−10896

the 50% cytotoxic concentration (CC_{50}) of compound **D163** was approximately 10 μM, and the compound displayed no antiviral activity at the maximum noncytotoxic concentration (Table 1). In the absence of a substituent in the NH_2 group (compound **D27**), the cytotoxic effect appeared already at a 0.1 μM concentration. However, insertion of a trifluoromethyl substituent R^2 into the meta position of the phenyl ring (**D119**) did not increase cytotoxicity, but EC_{50} of this compound remained higher compared to that of **D160**. A similar effect was also achieved by introducing a cyclopentyl substituent into the NH_2 group (**D164**), but such substitution had no significant effect on the antiviral activity of the compound. There was also no significant change in the activity when the position of the methyl groups R^2 in the phenyl ring was varied, while the substituent in the NH_2 group remained the same. Thus, for example, the activity of the **D165** analogue remained at the same level as that of **D159**, but at the same time, the trifluoromethyl group R^2 at the meta position of the phenyl in the arylglycine residue and the fluorine substituent R^1 at the meta position of the phenyl in cyclopropane ring led to the complete loss of the activity (**D166**). Probably, the loss of the activity of compound **D166** was due to a significant steric hindrance, which prevents the optimal binding of the ligand to the active center of CHIKV nsP2. It should be also noted that despite its structural similarity to **D119**, compound **D162** showed three times less antiviral activity than compound **D119** (EC_{50} = 95.9 and 32.0 μM, respectively; Table 1). Based on these results, it can be assumed that the position of the methyl groups (R^1) in the phenyl ring of the cyclopropane moiety (Scheme 1) has also a significant effect on the antiviral activity.

Subsequently, to study the effect of the stereochemical configuration on the antiviral activity, four stereoisomers of compound **D160**, exhibiting the highest antiviral activity, were synthesized: **D160a−d** (Scheme 2; see the Supporting Information). All stereoisomers showed different activity against CHIKV. In both pairs of diastereoisomers, **D160a** and **D160b** (*R,R,S*- and *R,R,R*-stereoisomers, respectively) and **D160c** and **D160d** (*S,S,R*- and *S,S,S*-stereoisomers, respectively), the most active stereoisomers had the *S*-configuration of the stereocenter in arylglycine (**D160a** and **D160d**). Surprisingly, the antiviral activity was almost the same in the pair of *S,S*-cyclopropane diastereoisomers (**D160c** and **D160d**), while the change of the configuration of the stereocenter in arylglycine in the pair of *R,R*-stereoisomers significantly altered their antiviral activity (Table 1).

Determination of Inhibitory Activities Using the Cell-Free Protease Assay. Compounds with the highest antiviral activity were selected for the cell-free protease inhibition assay—**D119**, **D127**, **D161**, and the stereoisomers **D160a−d**. Compounds **D119**, **D127**, and **D161** were tested as equimolecular mixtures of four possible stereoisomers. As is evident from increased amounts of the uncleaved substrate, all selected compounds inhibited the protease activity of nsP2 (Figure 4). However, in general, the effect on recombinant nsP2 was modest and only the stereoisomer **D160a** demonstrated strong inhibitory activity, as can be seen from the near absence of the cleavage product.

Molecular Docking and MD Simulations of Synthesized Compounds. Molecular docking at both potential binding sites of the nsP2 protease was performed with the *S,S,S*-stereoisomers of all synthesized compounds and with four individual stereoisomers of the most active compound

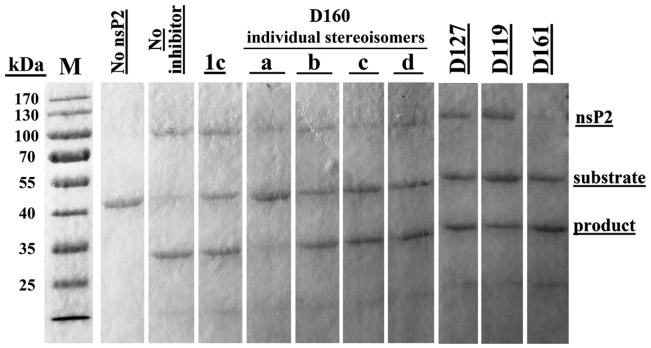

Figure 4. Effects of selected compounds (1 mM) on the protease activity of CHIKV nsP2. The image combines two gels. The gels were transferred on the paper before scanning. Compounds **D119**, **D127**, and **D161** represent equimolecular mixtures of four possible stereoisomers. The experiment was repeated three times, with very similar results.

D160 (**D160a−d**). The molecular docking results are presented in Table 2. The calculated binding energies of the *S,S,S*-stereoisomers of compounds **D27**, **D119**, **D127**, and **D159** and compounds **D161−D166** were in the range of −9.1 to −7.1 kcal/mol for potential binding site **1** and in the range of −8.5 to −6.9 kcal/mol for potential binding site **2**. The calculated binding energies of the individual stereoisomers **D160a−d** were in the range of −8.8 to −7.6 kcal/mol for potential binding site **1** and in the range of −9.2 to −8.8 kcal/mol for potential binding site **2**. A comparison of the binding modes of the *S,S,S*-stereoisomer of the inactive compound **D159** and the highest activity stereoisomer **D160d** at potential binding site **1** does not explain the absence of the antiviral activity of compound **D159** as their binding modes are almost identical. Both compounds form hydrogen bonds with the OH group of Tyr1079 (Figure 5A,B). In addition, compound **D160d** forms a hydrogen bond with the carbonyl group of the side chain of Asn1082 (Figure 5B). At the same time, the analysis of the binding modes of these compounds shows a significant difference in the positions of the ligands at potential binding site **2**. The *S,S,S*-stereoisomer of compound **D159** forms only hydrophobic contacts with CHIKV nsP2 (Figure 5C), while compound **D160d** forms a hydrogen bond with Leu1203 (Figure 5D), which is part of the loop between the β7 strand and the α9 helix, which in turn plays a key role in the recognition and binding of the substrate.[21]

The further study was focused on molecular docking and MD simulations of the stereoisomers **D160a−d**. During the molecular docking procedure, bonds in the ligands were fixed in their respective spatial configuration. A comparison of the calculated binding energies shows that the values of both binding sites are the same for the stereoisomers **D160a** and **D160d** (Table 2), while for the stereoisomers **D160b** and **D160c**, the best value is rather typical for potential binding site **2** (the difference with potential binding site **1** is 1.2 kcal/mol). The stereoisomers **D160a** and **D160d** were selected for further study using MD simulations. The MD simulations with a length of 50 nanoseconds (ns) were performed for both stereoisomers at both potential binding sites. In the case of the stereoisomer **D160a**, its complex with CHIKV nsP2 at potential binding site **2** was more stable compared to potential binding site **1** (Figure S1A,C). In the case of the stereoisomer **D160d**, the root-mean-square deviations (rmsds) of its complexes with the nsP2 protease at both potential binding

https://doi.org/10.1021/acsomega.1c00625
ACS Omega 2021, 6, 10884−10896

Table 2. Calculated Binding Energies, Ligand Efficiencies, and Binding Modes of Synthesized Compounds to CHIKV nsP2

		binding site 1			binding site 2		
code	absolute configuration of stereocenters	ΔG (kcal/mol)	LE[a]	interactions (H-bonds)	ΔG (kcal/mol)	LE[a]	interactions (H-bonds)
D27	*S*,*S*,*S*	−9.1	0.35	Cys1013, Ala1046, Tyr1079 (HO···HN, HO···H_2N), Asn1082 (O(carbonyl)···H_2N), Trp1084, Leu1205	−8.0	0.30	Gln1039, Lys1045, Leu1203, Glu1204 (COO^-···H_2N), Pro1224, Asp1235, Lys1239
D119	*S*,*S*,*S*	−9.0	0.31	Cys1013, Ala1046, Tyr1079, Asn1082, Trp1084, Leu1205	−6.9	0.23	Lys1045, Pro1191, Glu1204, Ile1221, His1222, Pro1224, Lys1239, Met1242, Leu1243
D127	*S*,*S*,*S*	−9.0	0.31	Cys1013, Ala1046, Tyr1079 (HO···HN, HO···H_2N), Asn1082 (O(carbonyl)···H_2N), Trp1084, Leu1205	−8.5	0.29	Gln1039, Lys1045, Leu1203, Glu1204 (COO^-···H_2N), Ile1221, Pro1224, Asp1235, Lys1239, Leu1243
D159	*S*,*S*,*S*	−7.1	0.19	Asn1011, Cys1013, Ser1048, Tyr1079 (HO···HN), Asn1082, Trp1084, Leu1205, Gln1241, Met1242, Asp1246	−7.5	0.20	Lys1045, Pro1191, Val1194, Leu1203, Glu1204, Lys1239, Leu1243
D160a	*R*,*R*,*S*	−8.8	0.27	Tyr1079, Asn1082, Trp1084, Lys1091, Met1242	−9.0	0.27	Pro1191, Leu1203, His1222, Lys1239
D160b	*R*,*R*,*R*	−7.6	0.23	Ser1048, Tyr1079 (HO···HN(substituted terminal group)), Trp1084, Lys1091, Met1242, Asp1246	−8.8	0.27	Lys1045, Pro1191, Leu1203, Ile1221, His1222, Met1238, Lys1239
D160c	*S*,*S*,*R*	−8.0	0.24	Asn1011, Cys1013, Ala1046, Tyr1047, Tyr1079, Asn1082, His1083, Trp1084, Asn1202, Glu1204, Leu1205	−9.2	0.28	Lys1045, Pro1191, Leu1192, Leu1203, Ile1221, His1222, Lys1239, Leu1243
D160d	*S*,*S*,*S*	−8.8	0.27	Cys1013, Ala1046, Tyr1079 (HO···HN, HO···HN(substituted terminal group)), Asn1082 (O(carbonyl)···HN(substituted terminal group)), Trp1084, Leu1205, Met1242	−8.9	0.27	Pro1191, Leu1192, Leu1203 (NH(peptide)···O(carbonyl)), Glu1204, Met1238, Lys1239, Met1242
D161	*S*,*S*,*S*	−7.6	0.25	Asn1011, Cys1013, Ala1046, Tyr1079, Asn1082, Trp1084, Asn1202, Glu1204, Leu1205, Met1242	−7.6	0.25	Gly1176, Pro1191, Ile1221, His1222, Lys1239, Leu1243
D162	*S*,*S*,*S*	−8.2	0.29	Asn1011, Cys1013, Ala1046, Tyr1047, Tyr1079, Asn1082 (O(peptide)···H_2N), Trp1084, Asn1202, Glu1204, Met1242	−7.6	0.27	Lys1045, Leu1192, Leu1203, Glu1204 (COO^-···H_2N), Ile1221, Lys1239, Met1242, Leu1243
D163	*S*,*S*,*S*	−8.1	0.28	Ala1046, Tyr1047, Ser1048, Tyr1079, Trp1084, Lys1091, Leu1205, Gln1241, Met1242	−7.5	0.26	Lys1045, Leu1203, Ile1221, His1222, Lys1239, Leu1243
D164	*S*,*S*,*S*	−8.1	0.26	Ser1048, Tyr1079, Trp1084	−8.1	0.26	Pro1191, Leu1192, Leu1203 (NH···O(carbonyl)), Glu1204, Ile1221, Lys1239, Leu1243
D165	*S*,*S*,*S*	−8.0	0.21	Cys1013, Ala1046, Tyr1047, Ser1048, Tyr1079, Asn1082, Trp1084, Gln1241, Met1242	−8.0	0.21	Lys1045, Pro1191, Val1194, Leu1203, Ile1221, Lys1239, Leu1243
D166	*S*,*S*,*S*	−8.4	0.21	Ala1046, Tyr1079, Asn1082, Trp1084, Lys1091, Met1242	−8.4	0.21	Lys1045, Val1194, Leu1203, Ile1221, Lys1239, Leu1243

[a]LE: ligand efficiency, that is, ΔG/N (heavy atoms).

https://doi.org/10.1021/acsomega.1c00625
ACS Omega 2021, 6, 10884−10896

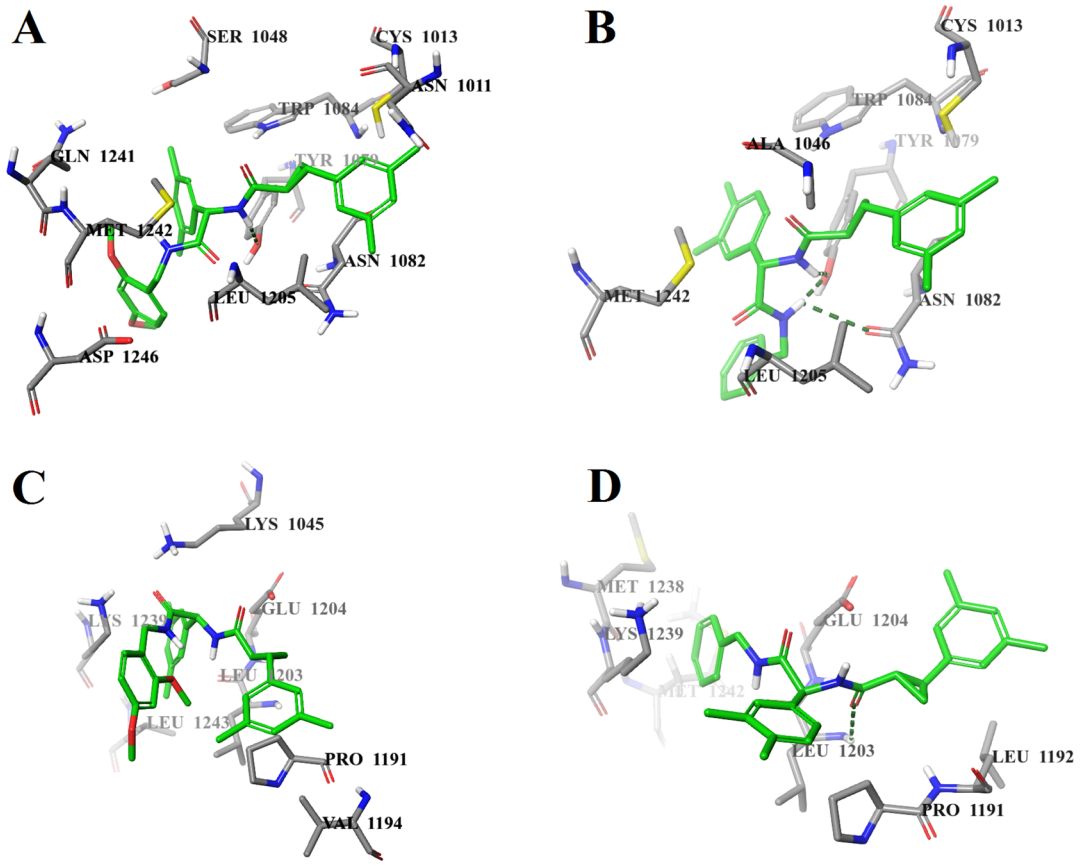

Figure 5. Calculated binding modes of (A) *S*,*S*,*S*-stereoisomer of **D159** at potential binding site **1** of CHIKV nsP2, (B) *S*,*S*,*S*-stereoisomer **D160d** at potential binding site **1** of CHIKV nsP2, (C) *S*,*S*,*S*-stereoisomer of **D159** at potential binding site **2** of CHIKV nsP2, and (D) *S*,*S*,*S*-stereoisomer **D160d** at potential binding site **2** of CHIKV nsP2 (PDB ID: 3TRK). Intermolecular hydrogen bonds are shown by dark-green dashed lines.

sites were approximately similar (Figure S1B,D). Analysis of the MD trajectory at potential binding site **1** showed that both stereoisomers do not form any contacts with the amino acid residues from the catalytic dyad of the CHIKV nsP2 protease, but the stereoisomer **D160a** forms a long-term stacking (π–π) interaction with the side chain of the conserved amino acid residue Trp1084 (Figure 6A). The stereoisomer **D160d**, in turn, forms two long-term contacts—a hydrogen bond and a stacking (π–π) interaction with the side chain of Tyr1079 as well as a water bridge with the backbone of Glu1204 (Figure 6B). Thus, based on the MD results for potential binding site **1**, it can be assumed that the stereoisomer **D160a** may have the highest antiviral activity due to a specific hydrophobic contact with the side chain of the conserved amino acid residue Trp1084, which is important for the activity of the nsP2 protease.[18] However, experimental data show that the activity of the stereoisomer **D160a** in the cell-based assay is almost 6 times lower than the activity of **D160d**, 26.8 and 4.8 μM, respectively (Table 1). According to the MD results, the binding of both stereoisomers at potential binding site **2** is more specific than that at potential binding site **1**. The stereoisomer **D160a** has two long-term contacts—a hydrogen bond with the backbone of His1222 and a hydrogen bond with the backbone of Lys1239, in addition to a short-term π-cation interaction with the side chain of Lys1239 as well as nonspecific hydrophobic interactions with Pro1191, Val1194, Leu1203, Ile1221, Leu1243, and Pro1224 (Figure 6C). The stereoisomer **D160d** forms several long-term contacts—a hydrogen bond and a water bridge with the backbone of Leu1203, two hydrogen bonds and several water bridges with Glu1204, and three π-cation interactions with Lys1045 and Lys1239 (Figure 6D). As can be seen from these data, the stereoisomer **D160d** remains bound to the amino acid residues of the loop between the β7 strand and the α9 helix (Leu1203, Glu1204, and Leu1205), which probably block the conformational changes of the CHIKV nsP2 protease required for substrate recognition and binding.[21] It is worth noting that **D160d** binds to these amino acid residues at both potential binding sites, indicating that the most likely mechanism of its action is associated with blocking the binding of the substrate rather than the catalytic dyad.

Evaluation of Antiviral Activity at High MOI. The antiviral activity of the two stereoisomers, **D160a** and **D160d**, and compound **D161** (an equimolecular mixture of four possible stereoisomers) was also analyzed using cells infected at MOI 10. Under these conditions, CHIKV infection is rapid and unlike low MOI infection, there is no spread of the virus from infected cells to noninfected cells. In this experiment, the inhibition of CHIKV infection was monitored by evaluation of the expression of CHIKV nsP1, nsP2, and capsid proteins (Figure 7). In this assay, compounds **D160a** and **D161** exhibited the dose-dependent antiviral activity at a concentration greater than 50 μM, down-regulating production of viral nsP1 and nsP2 as well as capsid protein. The fact that inhibition required concentrations slightly above EC_{50} of the compounds (26.8 and 13.9 μM, respectively; Table 1) can be attributed to lower sensitivity of the assay performed at high MOI. Interestingly, in the case of the stereoisomer **D160d**, a

https://doi.org/10.1021/acsomega.1c00625
ACS Omega 2021, 6, 10884−10896

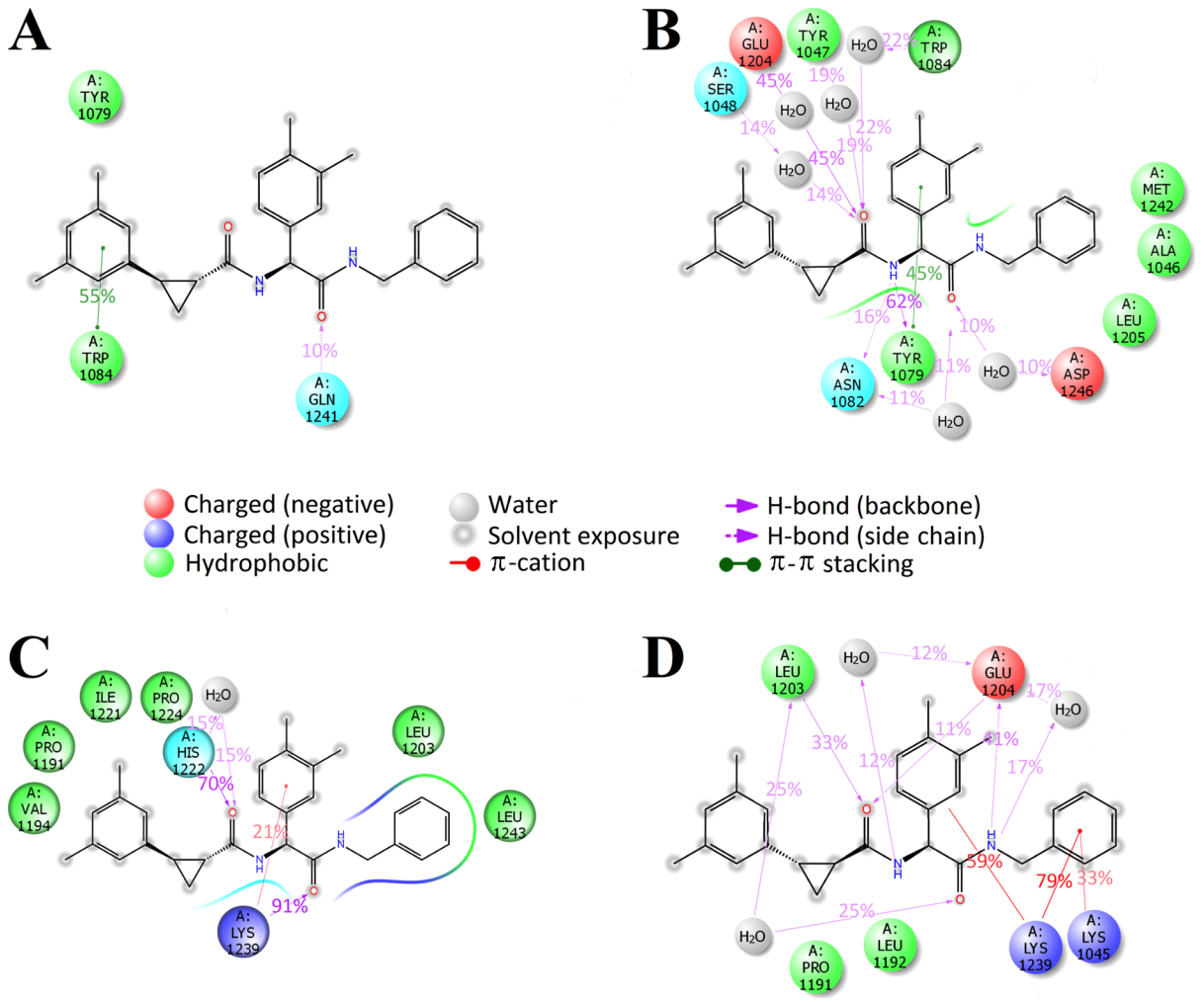

Figure 6. MD-calculated contacts of (A) *R,R,S*-stereoisomer **D160a** at potential binding site **1** of CHIKV nsP2, (B) *S,S,S*-stereoisomer **D160d** at potential binding site **1** of CHIKV nsP2, (C) *R,R,S*-stereoisomer **D160a** at potential binding site **2** of CHIKV nsP2, and (D) *S,S,S*-stereoisomer **D160d** at potential binding site **2** of CHIKV nsP2 (PDB ID: 3TRK). Interactions that occur more than 10% of the simulation time are shown.

slight decrease in the production of viral proteins was observed only at a concentration of 200 μM, a concentration much higher of EC_{50} (4.8 μM; Table 1). As the main difference of assays performed at low and high MOI is the presence of viral spread at the former case, it could be speculated that antiviral effects of the stereoisomer **D160d** may include inhibition of virion formation and/or release. Such an effect has been observed for deletion of residues 998−1003 of CHIKV ns-polyprotein; these residues are located close to the active site of the nsP2 protease.[22] Additional studies are required to reveal whether the addition of the stereoisomer **D160d** mimics the effect of these mutations.

CONCLUSIONS

In this work, the structure and antiviral properties of the previously found CHIKV nsP2 protease inhibitor[13] were optimized using CADD methods, synthesis, and cell-based and cell-free experiments. Based on the structure of CHIKV nsP2 inhibitor **1c** discovered in our previous study,[13] 158 novel analogues were designed, and 11 novel derivatives were synthesized and tested for their ability to inhibit both the enzymatic activity of the nsP2 protease and the replication of the virus as a whole. By optimizing the structure of the inhibitor, a series of compounds with antiviral activity 2−10 times higher than that of the initial compound **1c** were obtained. The results of molecular modeling of the binding of the studied potential inhibitors showed that the most probable mechanism of inhibition of the CHIKV nsP2 protease activity is the blocking of conformational changes in nsP2 required for substrate recognition and binding. A study of the antiviral activity of the individual stereoisomers of the most active compound **D160** showed that the antiviral activity significantly depends on the spatial configuration of all stereocenters of the compound, and the *S,S,S*-configuration of stereocenters is preferred. However, it is worth noting that despite the high antiviral activity in the cell-based assay at a low MOI, the stereoisomer **D160d** did not show significant inhibitory activity in the cell-free protease assay and the cell-based assay at a high MOI. The opposite situation was observed in the case of the stereoisomer **D160a**, showing the greatest inhibitory effect both in the cell-free protease assay and in the cell-based assay at a high MOI. This difference can probably be explained by the different bioavailability of these stereoisomers, but their mechanism of action needs to be further investigated for a more detailed explanation. Thus, both stereoisomers of compound **D160** can be considered as new scaffolds for further optimization and development of new effective targeted inhibitors of CHIKV.

https://doi.org/10.1021/acsomega.1c00625
ACS Omega 2021, 6, 10884−10896

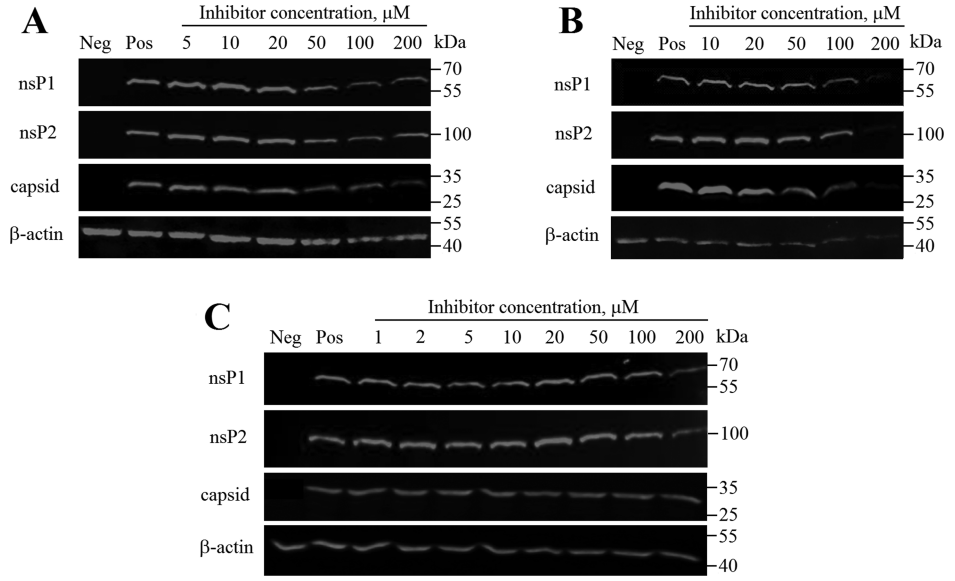

Figure 7. Western blot analysis of proteins from CHIKV-infected cells that were treated using compounds **D160a** (*R,R,S*-stereoisomer) (A), **D161** (an equimolecular mixture of four possible stereoisomers) (B), and **D160d** (*S,S,S*-stereoisomer) (C). BHK-21 cells infected with CHIKV-NanoLuc (MOI 10) were treated with increasing concentrations of the inhibitor. Cell lysates were collected 6 h post infection; proteins were separated using SDS-PAGE, transferred onto the PVDF membrane, and detected using indicated antibodies. *β*-Actin was detected as the loading control. Names of the proteins are indicated on the left; molecular masses of marker bands are indicated on the right. Neg—mock-infected BHK-21 cells treated with 1% DMSO; Pos—CHIKV-infected BHK-21 cells treated with 1% DMSO (no inhibitor).

MATERIALS AND METHODS

Molecular Modeling. *Target.* The crystal structure of the CHIKV nsP2 protease (PDB ID: 3TRK)[15] was used for molecular docking. The structural model was measured by X-ray diffraction with a resolution of 2.40 Å. The raw crystal structure was corrected, and hydrogen atoms were automatically added to the protein using Schrödinger's Protein Preparation Wizard of Maestro 10.7.[23] All selenomethionines were converted to methionines. Water molecules were removed from the crystal structure.

Small-Molecule Library. The two-dimensional chemical structures of the *S,S,S*-stereoisomers of designed compounds were drawn using Schrödinger's 2D Sketcher of Maestro. The ligand structures were prepared for molecular docking using LigPrep with the OPLS_2005 force field from the Schrödinger Suite.[24] Generation of all possible states and ionization states was enumerated for each ligand using Epik at a pH of 7.0 ± 2. The stereoisomers were determined from the three-dimensional structures. PDB files for the molecular docking procedure were created from lowest-energy conformers for each ligand.

Molecular Docking. AutoDock Vina 1.1.2[25] was used for the docking studies to find out binding modes and binding energies of the *S,S,S*-stereoisomers of designed compounds to the receptor. In this study, two possible binding sites of the CHIKV nsP2 protease were selected for molecular docking. Potential binding site **1** of CHIKV nsP2 was specified with the residues Cys1013, His1083, and Trp1084 and was surrounded by a grid box sized 20 × 20 × 20 points with a spacing of 1.000 Å. Potential binding site **2** was specified with the residue His1222 and was surrounded by a grid box sized 24 × 24 × 24 points with a spacing of 1.000 Å. In the previously published work,[13] it was reported that the configuration of the cyclopropane fragment of compound **1c** was important for the antiviral activity; therefore, the cyclopropane bonds were fixed in *trans*-configuration for all compounds. The docking parameters were used in their default values, that is, one central processing unit to use, the number of output poses is 9, and the exhaustiveness is 8.

Molecular Dynamics. The MD simulations were carried out using the Desmond simulation package of Schrödinger LLC.[26] In all runs, the NPT ensemble (isothermal−isobaric) was applied with the temperature of 300 K and a pressure of 1 bar. The simulation lengths were 50 ns with a relaxation time of 1 picosecond (ps). The OPLS_2005 force field parameters were used in all simulations.[27] The long-range electrostatic interactions were calculated using the particle mesh Ewald method.[28] The cutoff radius in Coulomb interactions was 9.0 Å. The water molecules were described using the simple point charge model.[29] The Martyna−Tuckerman−Klein chain coupling scheme[30] with a coupling constant of 2.0 ps was used for the pressure control, and the Nosé−Hoover chain coupling scheme[30] was used for the temperature control. Nonbonded forces were calculated using an reversible reference system propagation algorithm integrator where the short-range forces were updated every step and the long-range forces were updated every three steps. The trajectories were saved at a 50.0 ps interval for analysis. The behavior and interactions between the ligands and protein were analyzed using the Simulation Interaction Diagram tool implemented in the Desmond MD package.

Cell Lines and Virus Strain. Baby hamster kidney (BHK-21) cells (ATCC CCL-10) were maintained in Glasgow's minimal essential medium (GMEM; PAN Biotech) containing 7.5% fetal bovine serum, 2% tryptose phosphate broth, 20 mM *N*-2-hydroxyethylpiperazine-*N*-ethanesulfonic acid (HEPES), and 1% penicillin/streptomycin. The cell culture was maintained at 37 °C in an atmosphere of 5% CO_2. The CHIKV-NanoLuc strain was obtained from the icDNA clone of pICRES1-NanoLuc, representing the LR2006OPY1 strain belonging to the East/Central/South African genotype.[31] The virus stocks were stored at −80 °C. All virus experiments were

https://doi.org/10.1021/acsomega.1c00625
ACS Omega 2021, 6, 10884−10896

conducted in accordance with the guidelines of the national authorities using appropriate biosafety laboratories under all necessary safety approvals.

Antiviral and Cytotoxicity Assays. *Compounds.* 10 mM stocks of compounds were prepared by dissolving compounds in sterile dimethyl sulfoxide (DMSO) (Sigma, USA) and stored at −20 °C until further use.

Antiviral Activity Assay. BHK-21 cells were seeded on 24-well tissue culture plates (Thermo Fisher Scientific) at a density 2 × 10^5 cells/well in 400 μL of GMEM and were allowed to adhere overnight. BHK-21 cells were infected with the CHIKV-NanoLuc virus at an MOI of 0.001 plaque-forming unit/cell in an infection medium (200 μM/well) containing GMEM, 0.2% bovine serum albumin (BSA), 1% of the penicillin/streptomycin stock, and compounds at final concentrations ranging from 0.1 to 100 μM. After 1 h post infection, a complete growth medium (300 μL/well) containing compounds at final concentrations ranging from 0.1 to 100 μM was added. At 16 h post infection, the medium was discarded, cells were lysed, and the activity of nanoluciferase was measured using a *Renilla* luciferase assay system (Promega). The assay was carried out in three parallels. EC_{50} calculation was performed using GraphPad Prism version 8.0 for Windows (GraphPad Software, La Jolla, California, USA).[32] The EC_{50} graphs are given in Figure S2.

Cytotoxicity Assay. BHK-21 cells were plated in 96-well plates containing the complete growth medium and were allowed to adhere overnight. The cells were then treated with compounds at the indicated concentrations and were incubated for 24 h. After 24 h of drug treatment, the cell viability was measured using the 3-(4,5-dimethylthiazol-2-yl)-2,5-diphenyl-2*H*-tetrazolium bromide (MTT) assay. Briefly, 10 μL of MTT solution (5 mg/mL) was added to each well and incubated at 37 °C for 4 h. After removing the medium, the crystals produced were dissolved in 100 μL of DMSO. The optical density of the solutions was measured at 540 nm. All experiments were performed in triplicate.

Cell-Free Protease Inhibition Assay. Full-length recombinant CHIKV nsP2 was used as the protease. The recombinant protein substrate contained the nsP2 cleavage site (residues P10 to P′5 from the nsP1/nsP2 cleavage site) placed between enhanced green fluorescent protein (EGFP) and thioredoxin. The recombinant proteins were expressed and purified, as described in detail earlier.[33,34] The protease inhibition assay was carried out at 30 °C for 1.5 h in a 10 μL volume in the protease assay buffer [20 mM HEPES (pH 7.2), 2 mM dithiothreitol]. The CHIKV nsP2 final concentration was 1.4 μM, the substrate's final concentration was 6 μM, and the inhibitor's final concentration was 1 mM; 10% DMSO was used as a solvent control. Protease inhibition assay reaction products (5.5 μL) were analyzed by 10% sodium dodecyl sulfate (SDS)-PAGE and Coomassie blue staining.

Western Blot Analysis. 90% confluent BHK-21 cells (1 × 10^6 cells/well in 35 mm diameter plates) were infected with CHIKV-NanoLuc at an MOI of 10 in the presence of the stereoisomers **D160a**, **D160d**, and compound **D161** in the infection medium (GMEM, 0.2% BSA, 20 mM HEPES). The stereoisomer **D160a** was tested at concentrations of 5 up to 200 μM, the stereoisomer **D160d** at concentrations of 1 up to 200 μM, and compound **D161** at concentrations of 10 up to 200 μM. Control cells were infected in the presence of 1% DMSO used as a solvent control. At 1 h post infection, the complete growth medium containing the same concentration of tested compounds or DMSO was added. Cells were incubated at 37 °C for 6 h, collected and lysed in 100 μL of the SDS sample buffer (50 mM Tris−HCl pH 6.8, 2% SDS, 10% glycerol, 0.2% bromophenol blue), and boiled at 100 °C for 8 min. Proteins were separated by SDS-PAGE in 10% gels and transferred onto hydrophilic polyvinylidene fluoride (PVDF) membranes. The CHIKV proteins were detected using the corresponding rabbit polyclonal antibodies (all generated in-house); β-actin (sc-47778; Santa Cruz Biotechnology) was used as a loading control. The membranes were incubated with the appropriate secondary antibodies conjugated to fluorescent infrared dyes (LI-COR), and the signals were visualized with the LI-COR Odyssey Fc Imaging System.

■ ASSOCIATED CONTENT

Supporting Information

The Supporting Information is available free of charge at https://pubs.acs.org/doi/10.1021/acsomega.1c00625.

Calculated binding energies of small-molecule ligands to the receptor CHIKV nsP2; description of the chemical synthesis of new potential inhibitors and copies of their ^1H and ^{13}C NMR spectra; rmsd of the atomic positions for the stereoisomers **D160a** and **D160d** with CHIKV nsP2; and determination of EC_{50} of the selected compounds in BHK-21 cells (PDF)

■ AUTHOR INFORMATION

Corresponding Authors

Andres Merits − *Institute of Technology, University of Tartu, 50411 Tartu, Estonia*; Email: andres.merits@ut.ee

Mati Karelson − *Institute of Chemistry, University of Tartu, 50411 Tartu, Estonia*; Email: mati.karelson@ut.ee

Authors

Larisa Ivanova − *Institute of Chemistry, University of Tartu, 50411 Tartu, Estonia*

Kai Rausalu − *Institute of Technology, University of Tartu, 50411 Tartu, Estonia*

Maksim Ošeka − *Department of Chemistry and Biotechnology, Tallinn University of Technology, 12618 Tallinn, Estonia*

Dzmitry G. Kananovich − *Department of Chemistry and Biotechnology, Tallinn University of Technology, 12618 Tallinn, Estonia*

Eva Žusinaite − *Institute of Technology, University of Tartu, 50411 Tartu, Estonia*

Jaana Tammiku-Taul − *Institute of Chemistry, University of Tartu, 50411 Tartu, Estonia*; orcid.org/0000-0002-8781-4861

Margus Lopp − *Department of Chemistry and Biotechnology, Tallinn University of Technology, 12618 Tallinn, Estonia*

Complete contact information is available at: https://pubs.acs.org/10.1021/acsomega.1c00625

Author Contributions

L.I. performed molecular docking and MD simulations; L.I., J.T.-T., and M.K. analyzed modeling results. L.I., K.R., and E.Ž. performed biological experiments; L.I., K.R., E.Ž., A.M., and M.K. analyzed experimental data. M.O., D.G.K., and M.L. designed and performed the chemical synthesis of the compounds. A.M. and M.K. coordinated the project. All

authors participated in the preparation of the manuscript and approved the final manuscript.

Notes

The authors declare no competing financial interest.

■ ACKNOWLEDGMENTS

The current work was financially supported by the EU European Regional Development Fund through the Centre of Excellence in Molecular Cell Engineering (project no. 2014-2020.4.01.15-0013), Estonia. D.G.K. and M.O. acknowledge support from Tallinn University of Technology (grant no. B58).

■ REFERENCES

(1) Caglioti, C.; Lalle, E.; Castilletti, C.; Carletti, F.; Capobianchi, M. R.; Bordi, L. Chikungunya virus infection: an overview. *New Microbiol.* **2013**, *36*, 211−227.
(2) Silva, L. A.; Dermody, T. S. Chikungunya virus: epidemiology, replication, disease mechanisms, and prospective intervention strategies. *J. Clin. Invest.* **2017**, *127*, 737−749.
(3) Weaver, S. C.; Osorio, J. E.; Livengood, J. A.; Chen, R.; Stinchcomb, D. T. Chikungunya virus and prospects for a vaccine. *Expert Rev. Vaccines* **2012**, *11*, 1087−1101.
(4) Subudhi, B.; Chattopadhyay, S.; Mishra, P.; Kumar, A. Current Strategies for Inhibition of Chikungunya Infection. *Viruses* **2018**, *10*, 235.
(5) Lahariya, C.; Pradhan, S. K. Emergence of chikungunya virus in Indian subcontinent after 32 years: A review. *J. Vector Borne Dis.* **2006**, *43*, 151−160.
(6) Burt, F. J.; Rolph, M. S.; Rulli, N. E.; Mahalingam, S.; Heise, M. T. Chikungunya: a re-emerging virus. *Lancet* **2012**, *379*, 662−671.
(7) Roth, A.; Hoy, D.; Horwood, P. F.; Ropa, B.; Hancock, T.; Guillaumot, L.; Rickart, K.; Frison, P.; Pavlin, B.; Souares, Y. Preparedness for Threat of Chikungunya in the Pacific. *Emerg. Infect. Dis.* **2014**, *20*, No. e130696.
(8) Muniaraj, M. Fading chikungunya fever from India: beginning of the end of another episode? *Indian J. Med. Res.* **2014**, *139*, 468−470.
(9) Khan, A. H.; Morita, K.; Parquet, M. D. C.; Hasebe, F.; Mathenge, E. G.; Igarashi, A. Complete nucleotide sequence of chikungunya virus and evidence for an internal polyadenylation site. *J. Gen. Virol.* **2015**, *83*, 3075−3084.
(10) Singh, S. K.; Unni, S. K. Chikungunya virus: host pathogen interaction. *Rev. Med. Virol.* **2011**, *21*, 78−88.
(11) Fros, J. J.; van der Maten, E.; Vlak, J. M.; Pijlman, G. P. The C-terminal Domain of Chikungunya Virus nsP2 Independently Governs Viral RNA Replication, Cytopathicity, and Inhibition of Interferon Signaling. *J. Virol.* **2013**, *87*, 10394−10400.
(12) Jadav, S. S.; Sinha, B. N.; Hilgenfeld, R.; Jayaprakash, V. Computer-Aided Structure Based Drug Design Approaches for the Discovery of new Anti-CHIKV Agents. *Curr. Comput.-Aided Drug Des.* **2017**, *13*, 346−361.
(13) Das, P. K.; Puusepp, L.; Varghese, F. S.; Utt, A.; Ahola, T.; Kananovich, D. G.; Lopp, M.; Merits, A.; Karelson, M. Design and Validation of Novel Chikungunya Virus Protease Inhibitors. *Antimicrob. Agents Chemother.* **2016**, *60*, 7382−7395.
(14) Bassetto, M.; De Burghgraeve, T.; Delang, L.; Massarotti, A.; Coluccia, A.; Zonta, N.; Gatti, V.; Colombano, G.; Sorba, G.; Silvestri, R.; Tron, G. C.; Neyts, J.; Leyssen, P.; Brancale, A. Computer-aided identification, design and synthesis of a novel series of compounds with selective antiviral activity against chikungunya virus. *Antiviral Res.* **2013**, *98*, 12−18.
(15) 3TRK: Structure of the Chikungunya virus nsP2 protease. *Research Collaboratory for Structural Bioinformatics Protein Data Bank*, Spetember 28, 2011. https://www.rcsb.org/structure/3TRK (accessed 2021-01-27). (b) Cheung, J.; Franklin, M.; Mancia, F.; Rudolph, M.; Cassidy, M.; Gary, E.; Burshteyn, F.; Love, J. Structure of the Chikungunya virus nsP2 protease. **2011** Unpublished work.
(16) Shityakov, S.; Foerster, C. In silico predictive model to determine vector-mediated transport properties for the blood−brain barrier choline transporter. *Adv. Appl. Bioinf. Chem.* **2014**, *7*, 23−36.
(17) Rashad, A. A.; Mahalingam, S.; Keller, P. A. Chikungunya Virus: Emerging Targets and New Opportunities for Medicinal Chemistry. *J. Med. Chem.* **2014**, *57*, 1147−1166.
(18) Rausalu, K.; Utt, A.; Quirin, T.; Varghese, F. S.; Žusinaite, E.; Das, P. K.; Ahola, T.; Merits, A. Chikungunya virus infectivity, RNA replication and non-structural polyprotein processing depend on the nsP2 protease's active site cysteine residue. *Sci. Rep.* **2016**, *6*, 37124.
(19) Moni, L.; Denißen, M.; Valentini, G.; Müller, T. J. J.; Riva, R. Diversity-Oriented Synthesis of Intensively Blue Emissive 3-Hydroxyisoquinolines by Sequential Ugi Four-Component Reaction/Reductive Heck Cyclization. *Chem.—Eur. J.* **2015**, *21*, 753−762.
(20) Thompson, M. J.; Chen, B. Ugi Reactions with Ammonia Offer Rapid Access to a Wide Range of 5-Aminothiazole and Oxazole Derivatives. *J. Org. Chem.* **2009**, *74*, 7084−7093.
(21) Narwal, M.; Singh, H.; Pratap, S.; Malik, A.; Kuhn, R. J.; Kumar, P.; Tomar, S. Crystal structure of chikungunya virus nsP2 cysteine protease reveals a putative flexible loop blocking its active site. *Int. J. Biol. Macromol.* **2018**, *116*, 451−462.
(22) Law, Y.-S.; Wang, S.; Tan, Y. B.; Shih, O.; Utt, A.; Goh, W. Y.; Lian, B.-J.; Chen, M. W.; Jeng, U.-S.; Merits, A.; Luo, D. Interdomain Flexibility of Chikungunya Virus nsP2 Helicase-Protease Differentially Influences Viral RNA Replication and Infectivity. *J. Virol.* **2021**, *95*, e01470−20.
(23) (a) Sastry, G. M.; Adzhigirey, M.; Day, T.; Annabhimoju, R.; Sherman, W. Protein and ligand preparation: parameters, protocols, and influence on virtual screening enrichments. *J. Comput.-Aided Mol. Des.* **2013**, *27*, 221−234. (b) *Schrödinger Suite 2020-4, Protein Preparation Wizard: Epik, Impact, and Prime*; Schrödinger, LLC: New York, NY, 2020.
(24) *Schrödinger Release 2020-4: LigPrep*; Schrödinger, LLC: New York, NY, 2020.
(25) Trott, O.; Olson, A. J. AutoDock Vina: improving the speed and accuracy of docking with a new scoring function, efficient optimization, and multithreading. *J. Comput. Chem.* **2010**, *31*, 455−461.
(26) (a) Bowers, K. J.; Chow, D. E.; Xu, H.; Dror, R. O.; Eastwood, M. P.; Gregersen, B. A.; Klepeis, J. L.; Kolossvary, I.; Moraes, M. A.; Sacerdoti, F. D.; Salmon, J. K.; Shan, Y.; Shaw, D. E. Scalable Algorithms for Molecular Dynamics Simulations on Commodity Clusters. *Proceedings of the 2006 ACM/IEEE Conference on Supercomputing*; IEEE, 2006; p 43. (b) *Schrödinger Release 2020-4: Desmond Molecular Dynamics System*; D. E. Shaw Research: New York, NY, 2020; *Schrödinger Release 2020-4: Maestro−Desmond Interoperability Tools*; Schrödinger: New York, NY, 2020.
(27) Banks, J. L.; Beard, H. S.; Cao, Y.; Cho, A. E.; Damm, W.; Farid, R.; Felts, A. K.; Halgren, T. A.; Mainz, D. T.; Maple, J. R.; Murphy, R.; Philipp, D. M.; Repasky, M. P.; Zhang, L. Y.; Berne, B. J.; Friesner, R. A.; Gallicchio, E.; Levy, R. M. Integrated Modeling Program, Applied Chemical Theory (IMPACT). *J. Comput. Chem.* **2005**, *26*, 1752−1780.
(28) Toukmaji, A. Y.; Board, J. A., Jr. Ewald summation techniques in perspective: a survey. *Comput. Phys. Commun.* **1996**, *95*, 73−92.
(29) Zielkiewicz, J. Structural properties of water: Comparison of the SPC, SPCE, TIP4P, and TIP5P models of water. *J. Chem. Phys.* **2005**, *123*, 104501. *J. Chem. Phys.* **2006**, *124*, 109901.
(30) Martyna, G. J.; Klein, M. L.; Tuckerman, M. Nosé-Hoover chains: The canonical ensemble via continuous dynamics. *J. Chem. Phys.* **1992**, *97*, 2635−2643.
(31) Utt, A.; Quirin, T.; Saul, S.; Hellström, K.; Ahola, T.; Merits, A. Versatile Trans-Replication Systems for Chikungunya Virus Allow Functional Analysis and Tagging of Every Replicase Protein. *PloS One* **2016**, *11*, No. e0151616.
(32) *GraphPad Prism for Windows*, ver. 8.0; GraphPad Software: La Jolla, CA, 2020; www.graphpad.com (accessed 2020-09-19).
(33) Das, P. K.; Merits, A.; Lulla, A. Functional cross-talk between distant domains of chikungunya virus non-structural protein 2 is

decisive for its RNA-modulating activity. *J. Biol. Chem.* **2014**, *289*, 5635−5653.
(34) Utt, A.; Das, P. K.; Varjak, M.; Lulla, V.; Lulla, A.; Merits, A. Mutations Conferring a Noncytotoxic Phenotype on Chikungunya Virus Replicons Compromise Enzymatic Properties of Nonstructural Protein 2. *J. Virol.* **2015**, *89*, 3145−3162.

https://doi.org/10.1021/acsomega.1c00625
ACS Omega 2021, 6, 10884−10896